THE EVOLUTION OF HELIUM AND HYDROGEN IONIZATION CORRECTIONS AS H II REGIONS AGE

Ruth Gruenwald[1], Gary Steigman[2], and Sueli M. Viegas[1]

[1]*Instituto Astronômico e Geofísico, Universidade de São Paulo, São Paulo, S.P. 04301-904, BRASIL*

[2]*Departments of Physics and Astronomy, The Ohio State University, Columbus, OH 43210, USA*

Abstract

Helium and hydrogen recombination lines observed in low-metallicity, extragalactic, H II regions provide the data used to infer the primordial helium mass fraction, Y_P. In deriving abundances from observations, the correction for unseen neutral helium or hydrogen is usually assumed to be absent; *i.e.*, the ionization correction factor is taken to be unity ($icf \equiv 1$). In a previous paper (VGS), we revisited the question of the icf for H II regions ionized by clusters of young, hot, metal-poor stars, confirming earlier work which had demonstrated a "reverse" ionization correction: $icf < 1$. In VGS the icf was calculated using more nearly realistic models of inhomogeneous H II regions, revealing that for those H II regions ionized by young stars with "hard" radiation spectra the icf is reduced even further below unity compared to homogeneous models. Based on these results, VGS suggested that the published values of Y_P needed to be reduced by an amount of order 0.003. As star clusters age, their stellar spectra evolve and so, too, will their icfs. Here the evolution of the icf is studied, along with that of two, alternate, measures of the "hardness" of the radiation spectrum. The differences between the icf for radiation-bounded and matter-bounded models are also explored, along with the effect on the icf of the He/H ratio (since He and H compete for some of the same ionizing photons). Particular attention is paid to the amount of doubly-ionized helium predicted, leading us to suggest that observations of, or bounds to, He^{++} may help to discriminate among models of H II regions ionized by starbursts of different ages and spectra. We apply our analysis to the Izotov & Thuan (IT) data set utilizing the radiation softness parameter, the [OIII]/[OI] ratio, and the presence or absence of He^{++} to find $0.95 \lesssim icf \lesssim 0.99$. This suggests that the IT estimate of the primordial helium abundance should be *reduced* by $\Delta Y \approx 0.006 \pm 0.002$, from 0.244 ± 0.002 to 0.238 ± 0.003.

1. Introduction

As the second most abundant element in the universe, whose abundance even today is dominated by its early universe production during Big Bang Nucleosynthesis (BBN), ^{4}He plays a key role in testing the consistency of the standard, hot, big bang model of cosmology and in using primordial nucleosynthesis as a probe of cosmology and particle physics (for a recent review and further references, see Olive, Steigman & Walker 2000). To minimize the unavoidable contamination from post-BBN production of ^{4}He, low-metallicity, extragalactic H II regions are the targets of choice for deriving the primordial abundance. Observations of large numbers of such H II regions have led to estimates of the primordial helium mass fraction, $Y_{\rm P}$, whose *statistical* uncertainties are very small, $\approx 1\%$ (*e.g.*, see, Olive & Steigman 1995 (OS), Olive, Skillman, & Steigman 1997 (OSS), Izotov, Thuan & Lipovetsky 1994, 1997 (ITL), Izotov & Thuan 1998 (IT), Peimbert, Peimbert, & Ruiz 2000 (PPR)). Now, more than ever before, it is crucial to attack potential sources of *systematic* error. In a previous paper (Viegas, Gruenwald, & Steigman 2000 (VGS)) we explored the size of the ionization correction for unseen neutral hydrogen and/or helium in H II regions ionized by young, hot, metal-poor stars. In VGS models of more nearly realistic, inhomogeneous H II region models were compared with the data set assembled by IT, leading to the conclusion that, on average, $icf < 1$ for the IT H II regions. Since IT (as well as almost all other analyses of H II region observations) *assumed* $icf \equiv 1$, VGS suggested that their derived value of $Y_{\rm P}$ needed to be reduced by ≈ 0.003, from $Y_{\rm P} \approx 0.244$ to $Y_{\rm P} \approx 0.241$. Some support for this lower value comes from the recent observations by PPR of a relatively metal-rich SMC H II region for which they derive Y(SMC)$= 0.2405 \pm 0.0017$, as well as from an independent theoretical study by Sauer & Jedamzik (2001; hereafter SJ).

In VGS models were calculated of H II regions ionized by the radiation from starbursts of two different ages (Cid-Fernandes *et al.* 1992): $t = 0$ and $t = 2.5$ Myr. The predictions for these two cases are in stark contrast, with $icf < 1$ for the young star cluster and $icf > 1$ for the older one. The difference is easy to understand as a consequence of the evolving radiation spectrum. The young star cluster has many massive, hot stars which produce a "hard" spectrum with many

helium-ionizing photons. As the star cluster ages, the more massive stars die, and the spectrum softens, reducing the relative number of helium to hydrogen ionizing photons. However, the evolution of the radiation spectrum from a cluster of stars is not monotonic. As time goes by, stellar winds strip away the atmospheres of lower mass stars exposing their hotter interiors and the resulting stellar spectra harden, producing relatively more He^0 and He^+ ionizing photons. Eventually, even these stars end their lives and the spectrum softens, the overall flux of ionizing radiation decreases, and the H II region fades away.

When comparing with the IT data, in order to distinguish between H II regions ionized by "hard" spectra for which $icf < 1$ and those ionized by "soft" spectra leading to $icf > 1$, VGS utilized the Vilchez-Pagel "radiation softness parameter" (Vilchez & Pagel 1998)

$$\eta \equiv (\frac{n(0^+)}{n(S^+)})(\frac{n(S^{++})}{n(O^{++})}), \tag{1}$$

finding that the IT data prefer a hard spectrum ($\log \eta \lesssim 0.4$), favoring a "reverse" ionization correction ($icf < 1$).

In this paper the evolution of model H II regions is studied tracking the changes in the icf, the radiation softness parameter η, the abundance of doubly ionized helium (He^{++}/H^+), and an alternate radiation softness parameter proposed by Ballantyne, Ferland, & Martin (2000; hereafter BFM), the ratio [OIII]λ5007/[OI]λ6300. In §2 we follow the evolution of the radiation spectrum using the starburst models of Cid-Fernandes *et al.* (1992), concentrating on the *relative* changes in the hydrogen and helium ionizing fluxes and their implications for the evolution of the icf, η, [OIII]/[OI], and the HeII(4686)/Hβ ratio. Since hydrogen and helium compete for the same ionizing photons, the sizes of the H^0 and He^0 zones may depend on the "true" He/H ratio. This effect is explored in §3. In §4 we model H II regions ionized by the composite spectra of starbursts of different ages, and investigate the observational consequences of superposed H II regions (see, also, VGS). Since it is the structure of the "outer" zones in an H II region which most influences the icf, in §5 the predictions of radiation-bounded and matter-bounded models are compared. Our results are discussed in §6 and our conclusions presented in §7.

2. Evolution of Starburst Spectra And The icf

Cid-Fernandes *et al.* (1992) explored the time-evolution of the radiation from starbursts of different total stellar masses. The models utilize the Maeder stellar evolution models and adopt a Salpeter IMF (slope = 1.35) with an upper mass limit of 130 $M_\odot$. In Figure 1 are shown the spectral flux distributions for a starburst of $10^6 M_\odot$ at five different times in its evolution: $t = 0.0$, 2.5, 3.3, 4.5, 5.4 Myr. To more clearly expose those aspects of these spectra which are key to understanding the evolution of the icf, in Figure 2 are shown the time-evolution of various ratios of the hydrogen (H^0) and helium (He^0, He^+) ionizing fluxes.

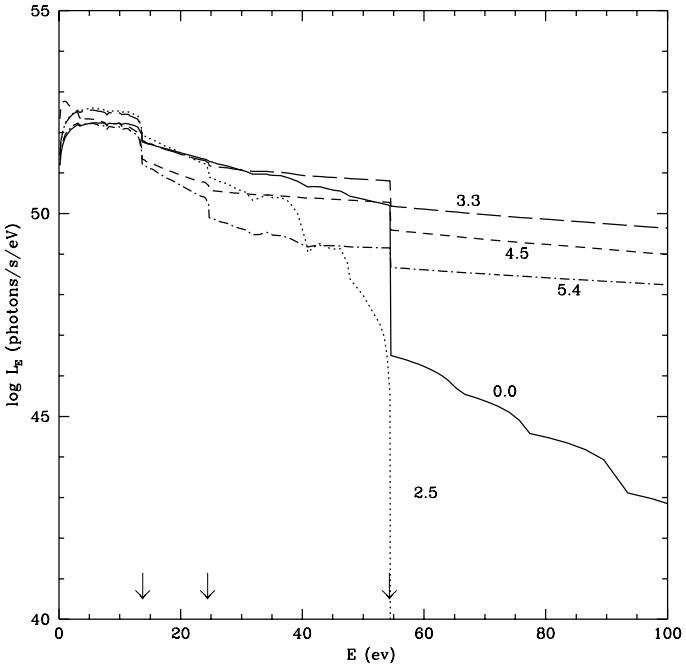

Fig. 1.— The spectral distribution (photons $s^{-1}eV^{-1}$) of the radiation from a $10^6 M_\odot$ starburst at five different epochs in its evolution: $t = 0$ (solid), 2.5 Myr (dotted), 3.3 Myr (long-dashed), 4.5 Myr (short-dashed), and 5.4 Myr (dot-dashed). The breaks in the spectra occur at the hydrogen and helium ionization edges, indicated by the arrows.

Initially, due to the presence of massive, hot stars, relatively large amounts of helium ionizing

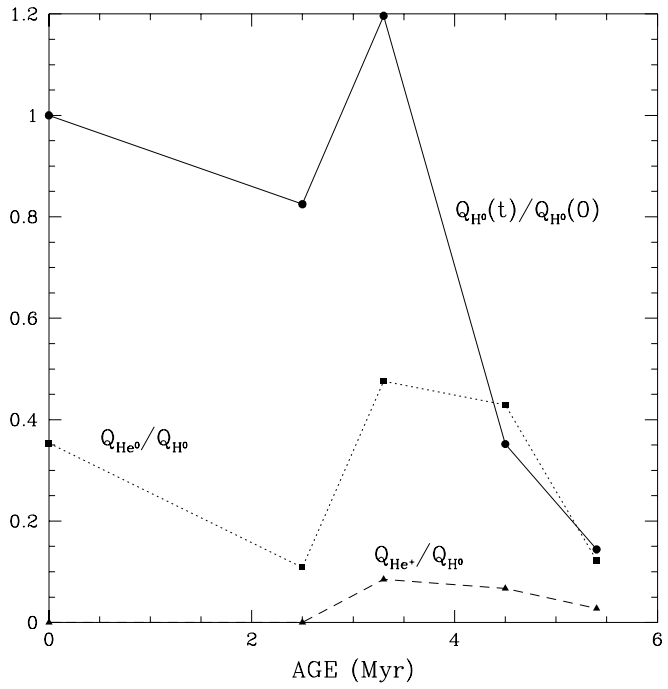

Fig. 2.— The evolution of the ionizing fluxes as the starburst ages. The solid line traces the evolution of hydrogen-ionizing photons ($E \geq 13.6$ eV). The dotted line follows the ratio of all He-ionizing ($E \geq 24.6$ eV) to H-ionizing fluxes, while the dashed line is the same for the He^+-ionizing photons ($E \geq 54.4$ eV) alone.

photons are present resulting, in general, in $icf < 1$ (see VGS). As the more massive stars evolve and die, the overall flux from the starburst decreases with the relative number of helium ionizing photons falling even faster, so that the icf increases and, by $t = 2.5$ Myr, $icf > 1$ (VGS). However, as the starburst continues to age, stellar winds strip away the atmospheres of the massive stars, exposing their hotter interiors. As a result, both the overall flux and the relative numbers of helium ionizing photons increase. In these more evolved H II regions ($t \sim 3$ Myr) the flux of He^+-ionizing photons is significant and detectable amounts of doubly-ionized helium should be present. As the star cluster continues to evolve, the overall flux of ionizing radiation decreases and so, too, does the ratio of helium-ionizing to hydrogen-ionizing photons. From Fig. 2 it can be anticipated that while a $\gtrsim 5$ Myr old H II region will have an $icf > 1$, similar to that of a

$\sim$ 2.5 Myr starburst, detectable amounts of He^{++} may be present in the former while absent in the latter, perhaps permitting an observational discrimination between the two.

2.1. Photoionization Models

Here, as in VGS, the AANGABA photoionization code (Gruenwald & Viegas 1992) is used to model the gas whose distribution is taken to be spherically symmetric and homogeneous. Since we are specifically interested in the helium – hydrogen *icf* for low-metallicity H II regions, a metal-poor chemical composition (0.1 solar) is chosen. Initially He/H = 0.083 (Y $\approx$ 0.25) is adopted, but later (§3) the consequences for the *icf* of different helium abundances are explored. The radiation intensity is characterized by the number of ionizing photons above the Lyman limit, Q_H, which is directly related to the mass and the IMF of the stellar cluster. Along with the gas density, n, Q_H defines the model H II regions. The popular ionization parameter, U, is proportional to Q_H/n, so that a grid of models at fixed density, characterized by different choices of U and R_i (the inner radius of the model H II region), corresponds to the identical grid labelled by *different* values of Q_H.

In VGS the *icf* (called "ICF" in that paper) was defined by relating the total He/H ratio to that of He^+/H^+ alone. As a result, any He^{++} was included along with unseen neutral H and He. However, lines from the recombination of He^{++} are observed in many H II regions, so that a more generally applicable definition, adopted in this paper, is

$$\frac{\mathrm{He}}{\mathrm{H}} \equiv icf \frac{(\mathrm{He^+} + \mathrm{He^{++}})}{\mathrm{H^+}}. \tag{2}$$

For H II regions with $He^{++} \ll He^+$, $icf \approx$ ICF, while in the presence of small, but observable amounts of He^{++}, $icf \lesssim$ ICF.

Using AANGABA, grids of model H II regions ionized by the radiation from starbursts of differing masses (*i.e.*, different Q_H), were created at each of the cluster ages identified above. In Figure 3 the results are shown in the *icf* – log η plane. As anticipated from Figures 1 and 2, $icf < 1$ for the hard spectra of the zero-age, 3.3, and 4.5 Myr starbursts, while $icf > 1$ for the

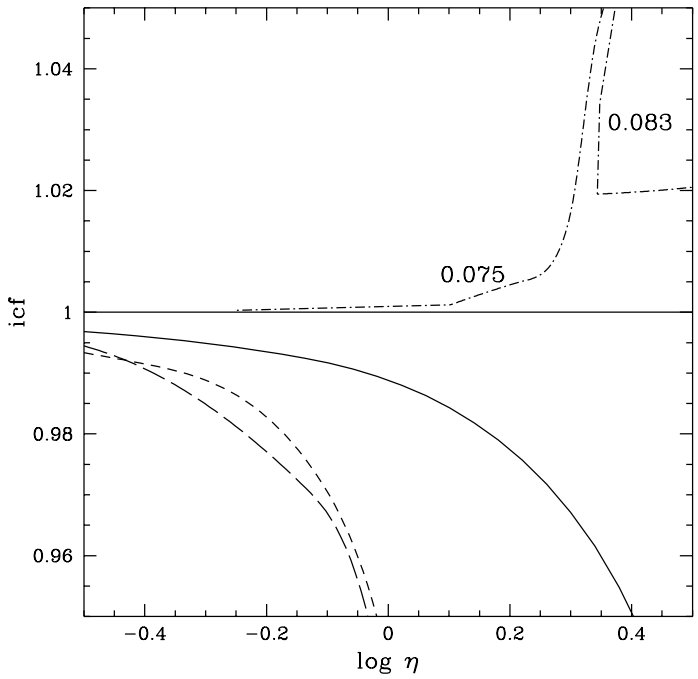

Fig. 3.— The icf (see eq. 2) versus the radiation softness parameter log η relations for H II regions of all ages ($0.0 \leq t \leq 5.4$ Myr). The solid line is for $t = 0$, the long-dashed line is for 3.3 Myr, the short-dashed line is for 4.5 Myr, and the dot-dashed lines are for 5.4 Myr. The 2.5 Myr model, for which log $\eta \gtrsim 0.8$, is off scale. The two curves for the 5.4 Myr starburst are for two choices of the helium abundance, He/H = 0.075 and 0.083 (see §3).

soft spectra of the 2.5 and 5.4 Myr models. Note that the 2.5 Myr starburst is offscale in Fig. 3 (where log $\eta \leq 0.5$) since for the very soft spectrum of this starburst, log $\eta \gtrsim 0.8$ (see VGS and Fig. 5); for the IT data, log $\eta \lesssim 0.4$. For the 5.4 Myr starburst the $icf - \eta$ relation depends on the helium abundance as discussed below in §3. For the $t = 0$, 3.3, 4.5 Myr models, and the 5.4 Myr model with He/H = 0.075, as the intensity of the starburst increases, η decreases and $icf \rightarrow 1$. In contrast, for the 5.4 Myr model with He/H = 0.083, as the intensity of the starburst increases, at first the icf *decreases* at nearly constant η, then η *increases* (to log $\eta \sim 0.6$) at nearly constant icf, and finally, as the size of the starburst is increased even further, η *decreases* (to log $\eta \sim 0.4$) as $icf \rightarrow 1$.

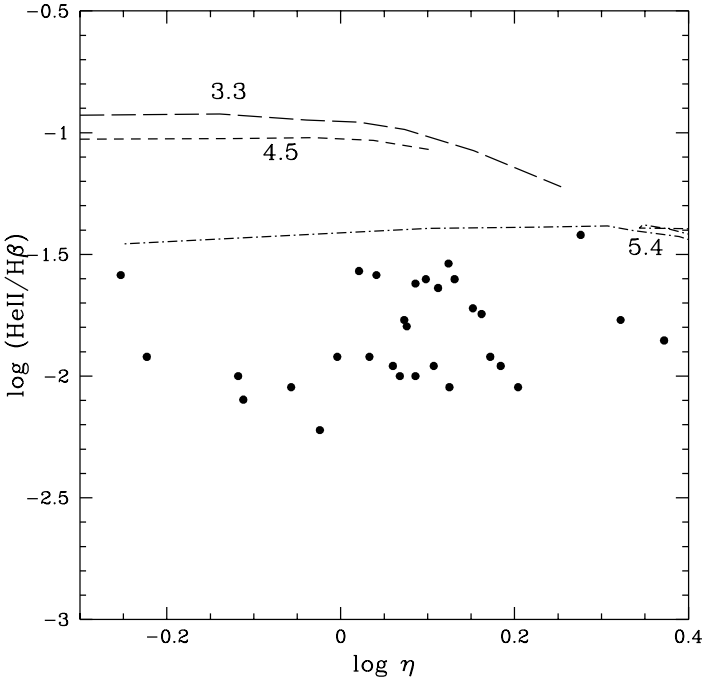

Fig. 4.— The HeII/Hβ ratio versus log η for H II regions of differing ages. The starburst ages are labelled on the curves. There are two dot-dashed curves for the 5.4 Myr starburst, corresponding to the two helium abundances (see Fig. 3). Note that for models of zero age and 2.5 Myr old starbursts, the predicted HeII emission is so small as to be off scale. The filled circles are the IT data.

In Figure 4 the model-predicted HeII(4686)/Hβ flux ratios are shown for starbursts of different ages, as a function of the radiation softness parameter η. Note that no curves appear for the zero-age and 2.5 Myr models because they predict that no detectable He^{++} should be present (at a level HeII/H$\beta \gtrsim 10^{-3}$). Also shown are the relevant data from IT who have detected He^{++} in $\sim$ 30 H II regions. It is noteworthy that *more* HeII(4686) is observed than is predicted for the young H II regions, while the opposite appears to be the case for the older H II regions. This strongly suggests that "real" H II regions may be ionized by a mixture of starbursts of different ages or, that what is observed could be the superposition of several H II regions within the telescope aperture (see VGS). If so, then the "true" *icf* must reflect some appropriately

weighted average of the various icfs shown in Figure 3. We return to this issue in §4, but note here that for the starburst spectrum employed by SJ, it is unlikely that any detectable He^{++} will be present. Clearly, the presence or absence of He^{++} can be a valuable clue to the hardness of the ionizing radiation spectrum. Before pursuing these issues, we first consider the alternative radiation softness parameter proposed by BFM.

2.2. An Alternate Radiation Softness Parameter?

There are advantages and disadvantages to using the Vilchez-Pagel radiation softness parameter η (see eq. 1). Since η requires the *ionic* ratios, it may be more convenient to employ a related parameter, similar to one introduced by Skillman (1989), which is simply a ratio of *line* ratios,

$$\eta' \equiv (\frac{I(\lambda 3727)}{I(\lambda 4959 + \lambda 5007)})(\frac{I(\lambda 6312)}{I(\lambda 6717 + \lambda 6731)}). \tag{3}$$

From our models we find that for the IT data range of $\log \eta < 0.4$, η' and η are closely related by,

$$\log \eta' = -1.82 + 0.88 \log \eta. \tag{4}$$

In our attempt to compare this with the IT *line* and *ionic* ratio data we have uncovered several inconsistencies between their line intensity ratios and their ionic ratios, which contribute to a spread around a best fit relation from the data of

$$\log \eta'(IT) = -1.85 + 0.76 \log \eta. \tag{5}$$

To facilitate comparison with previous analyses, in this paper we choose to utilize the original Vilchez-Pagel parameter η.

For the relatively hard spectra corresponding to starbursts of t = 0.0, 3.3, and 4.5 Myr, η decreases monotonically as the intensity of the starburst, Q_H, increases (*i.e.*, η and Q_H are anticorrelated). For these models there is also an anticorrelation between the icf (which is < 1) and η (see Fig. 3). In contrast, the η – Q_H and η – icf relations are *not* monotonic for the softer

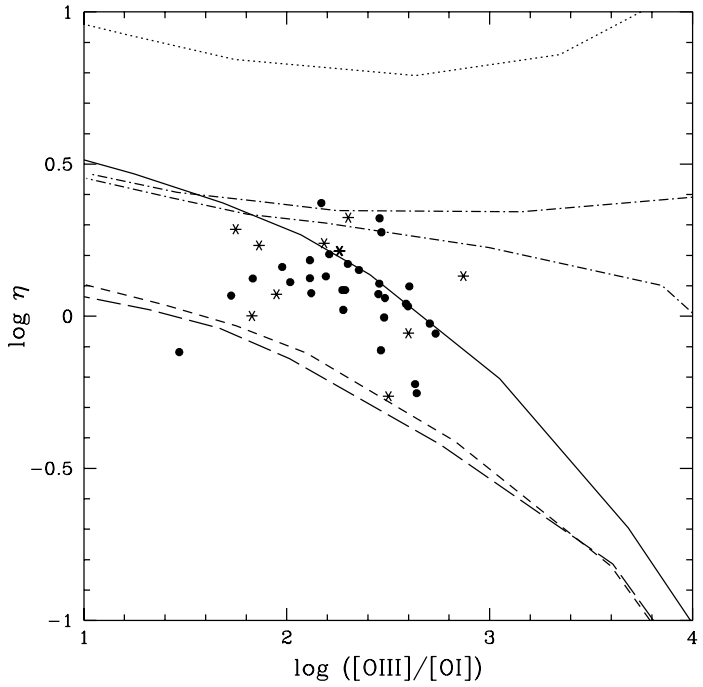

Fig. 5.— The radiation softness parameter η versus the [OIII]/[OI] ratio for H II regions of all ages (the line types are as in Figs. 1 and 3). Note that there are two curves (dot-dashed) for the 5.4 Myr models, corresponding to He/H = 0.075 (lower of the two) and 0.083 (see §3). The filled circles are the IT H II regions with observed He^{++}; the stars are for those regions without He^{++}.

spectra from starbursts of 2.5 and 5.4 Myr (for which $icf > 1$). Furthermore, for the latter starburst the character of the $icf - \eta$ relation changes with helium abundance.

BFM proposed an alternate radiation softness parameter, the ratio of [OIII]λ5007 to [OI]λ6300. This ratio of observed fluxes is independent of the H II region metallicity. We have tracked this ratio in our models and in Figure 5 the relationship between the Vilchez-Pagel radiation softness parameter, η, and the BFM parameter [OIII]/[OI], is shown for a series of H II region models ionized by starbursts of different ages. The variable along the curves is the intensity of the starburst, proportional to Q_H. For all starbursts as Q_H increases so, too, does the [OIII]/[OI] ratio. Figure 5 exposes a crucial difference between η and [OIII]/[OI]: whereas all spectra, whether "hard" or "soft", span the *entire* range in [OIII]/[OI], the ranges covered by η

are *different* for hard and soft spectra. While η may not be the ideal radiation softness parameter, the [OIII]/[OI] ratio has virtually no sensitivity to the spectral shape; rather, [OIII]/[OI] provides a measure of the *intensity* of the ionizing radiation field.

There is another problem if the [OIII]/[OI] ratio is used to provide an estimate of the hardness of the radiation spectrum. The [OI]λ6300 emission-line is produced in the recombination region, so its intensity is very dependent on the optical depth at the Lyman limit, τ_{LL}. We return to this point in §5, but simply remark here that for most models, the [OIII]/[OI] ratio decreases by more than 3 orders of magnitude as τ_{LL} increases from of order unity (matter-bounded) to of order 10^4 (radiation-bounded). In contrast, although the O^+ and S^+ fractions are each sensitive to τ_{LL}, η varies much less with τ_{LL} since it involves their *ratio* O^+/S^+.

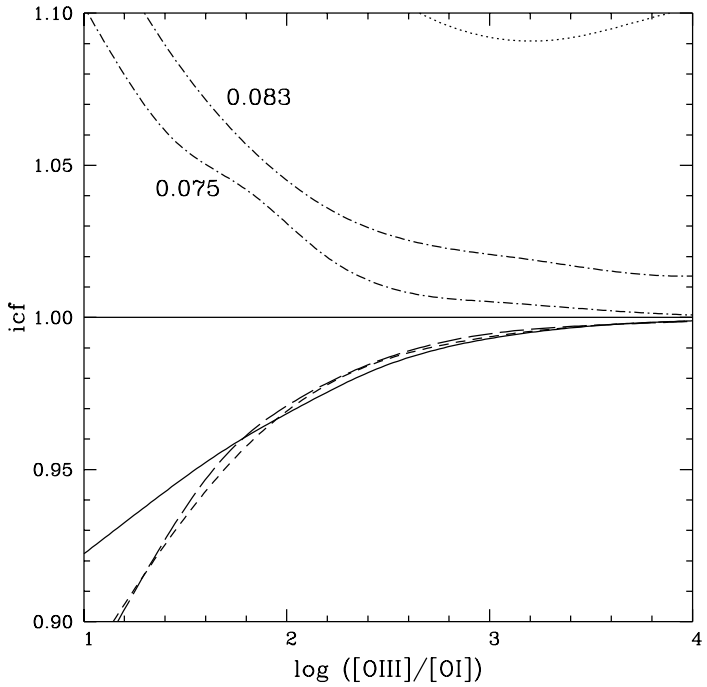

Fig. 6.— The *icf* versus the [OIII]/[OI] ratio for H II regions of all ages. The line types are as in Figs. 1, 3, and 5. The labels on the dot-dashed curves (5.4 Myr starburst) are the values of He/H.

The relevant IT data are also shown on Fig. 5. Notice that the IT H II regions, with $-0.3 \lesssim \log \eta \lesssim +0.4$, lie between the models for starbursts of all ages, but much below that for a 2.5

Myr starburst for which $\log \eta \gtrsim 0.8$. This suggests (see VGS) that starbursts of ≈ 2.5 Myr, with $icf > 1$, are not dominant in the H II regions observed by IT. The icfs for starbursts of differing ages are shown as a function of the [OIII]/[OI] ratio in Figure 6. Once again, notice that a measurement of the [OIII]/[OI] ratio does *not* determine either the size, or the sign, of the icf.

The predicted HeII/Hβ ratios are shown as a function of [OIII]/[OI] for starburst models of different ages in Figure 7. As was already seen in Fig. 4, no significant HeII is present in the young starbursts ($t \lesssim 2.5$ Myr), while higher than observed HeII/Hβ ratios are predicted for the older H II regions.

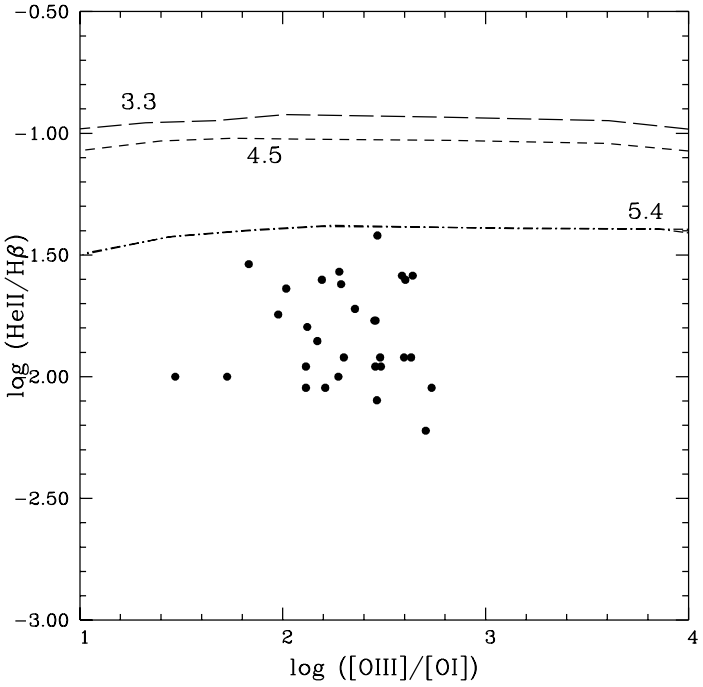

Fig. 7.— The HeII/Hβ ratio versus [OIII]/[OI] for H II regions of differing ages. The starburst ages are labelled on the curves. Note that for models of zero age and 2.5 Myr starbursts the predicted HeII emission is so small as to be off scale. The filled circles are from IT.

Although we are in agreement with BFM that the $icf \rightarrow 1.0$ as [OIII]/[OI] increases, we emphasize that for the [OIII]/[OI] range of the IT data ($1.4 \lesssim \log([\mathrm{OIII}]/[\mathrm{OI}]) \lesssim 2.9$), there are significant ionization corrections for starbursts of all ages. This is in contrast to the BFM

suggestion that $icf = 1$ when [OIII]/[OI] $\gtrsim 300$. At the same time, the Pagel *et al.* (1992) proposal that $icf = 1$ for $\log \eta < 0.9$ is unsupported by either our results (see Fig. 3) or those of SJ. For the η and [OIII]/[OI] ranges of the IT data, significant ionization corrections (at the few percent level) – most of them with $icf < 1$ – are to be expected (see, also, SJ).

3. The Effect Of The Helium Abundance On The Ionization Structure

Although models of the low metallicity H II regions targeted for determining the primordial helium abundance almost always adopt low heavy element abundances, little attention is usually given to the assumed helium abundance. For example, the helium abundance (by number) is He/H = 0.10 in Stasinska's (1990) models which were used by Pagel *et al.* 1992 to analyze their observed, low-metallicity H II regions. This helium abundance, Y $\approx$ 0.29, is even higher than the solar value (Bahcall, Pinsonneault, & Basu 2001). The Armour *et al.* (1999) and BFM analyses use the Orion abundance, He/H = 0.095 (Y $\approx$ 0.28). VGS set $Z = Z_{\odot}/10$ and chose He/H = 0.083 (Y $\approx$ 0.25).

Since helium competes with hydrogen for some of the same ionizing photons, the precise value of the helium abundance may affect the ionization structure of the H II region (Gruenwald & Viegas 2000). As we are tracking small deviations in the derived helium abundance, it is important to explore the effect of the adopted helium abundance on the model predictions of the icf, along with the other diagnostics such as η and the [OIII]/[OI] ratio. For starbursts of all ages model H II regions were computed for helium abundances varying from He/H = 0.075 (Y $\approx$ 0.23) to 0.10 (Y $\approx$ 0.29). From these models the following picture emerges.

The H II regions formed by massive starbursts (high Q_H) are large, with very thin transition zones, leading to an $icf \rightarrow 1$. For the more realistic starbursts (smaller Q_H), the He^0 and H^0 zones are larger and the icf deviates from unity, > 1 or < 1, depending on the hardness of the radiation spectrum. With the exception of the 5.4 Myr starburst, there are no significant variations of the icf (or of the other diagnostics) with He/H.

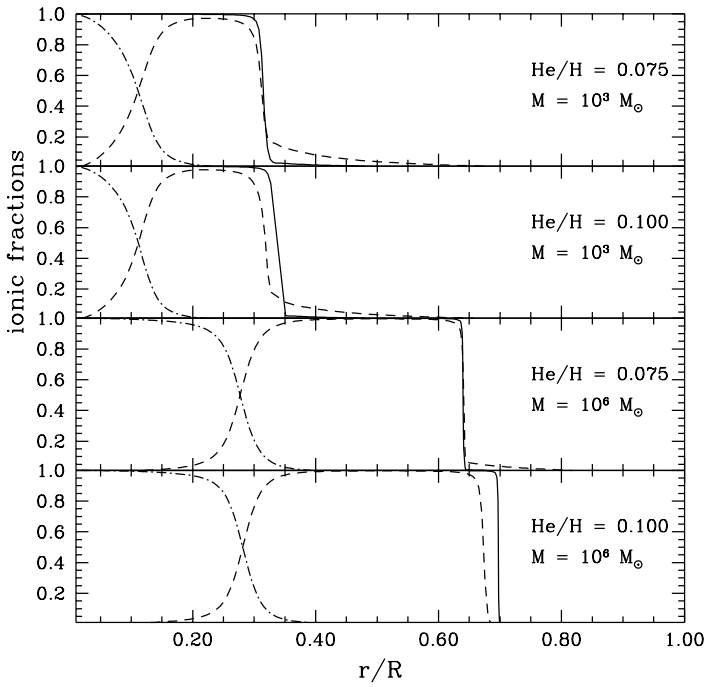

Fig. 8.— The radial distributions of the H^+ (solid), He^+ (dashed), and He^{++} (dot-dashed) fractions. R is the radius at which the H^+ fraction has dropped to 10^{-4}. The two upper panels are for a $10^3 M_\odot$ starburst and the two lower panels are for a $10^6 M_\odot$ starburst. In each pair of panels, the upper panel is for He/H = 0.075 and the lower one for He/H = 0.100.

For the softer spectra of the oldest starbursts ($\gtrsim$ 5 Myr) there are relatively fewer helium ionizing photons (see Fig. 2) and the corresponding H II regions have some neutral helium inside the ionized hydrogen zone so that $icf > 1$ (see Figs. 3 & 6). At fixed He/H, as the size of the starburst is reduced (smaller Q_H) the transition zone thickens and the *relative* contribution of He^0 increases, leading to an increase in the icf. At the same time, the [OIII]/[OI] ratio (which tracks Q_H) decreases, leading to an anticorrelation between the icf and [OIII]/[OI]. Now, at fixed Q_H, as the He/H ratio increases the [OIII]/[OI] ratio, which depends mainly on Q_H, is essentially unchanged, but the transition zone, where helium has become neutral while hydrogen is still ionized, grows in size since there is now more helium competing for the same ionizing photons. This effect is shown in Figure 8 where the radial distributions of the H^+, He^+, and He^{++}

fractions are shown for two choices of the size of the starburst ($M_* \approx 10^3 M_\odot$ and $M_* \approx 10^6 M_\odot$) and two choices for the helium abundance (He/H = 0.075, 0.100; Y ≈ 0.23, 0.29). For the smaller starburst, log([OIII]/[OI]) ≈ 2, while for the larger one, log([OIII]/[OI]) ≈ 3 for all values of He/H from 0.075 to 0.100. As a result, for a 5.4 Myr starburst, when the helium abundance increases the curves shift upwards in the icf – [OIII]/[OI] plane (see Fig. 6).

A much more dramatic change in the character of the curves occurs in the icf – η plane. For He/H $\lesssim$ 0.083, as Q_H increases *both* η and the icf decrease: η and the icf are positively correlated (while η and [OIII]/[OI] are slightly anticorrelated; see Fig. 5). In contrast, for He/H $\gtrsim$ 0.083 the variations of η and the icf with He/H, and with the size of the starburst, are non-monotonic. For these higher helium abundances (Y $\gtrsim$ 0.25), not entirely relevant to our study of low-metallicity H II regions, the structure of the transition zone is very sensitive to the precise helium abundance. For example, for the He/H = 0.083 case shown in Fig. 3, as Q_H increases from smaller to larger starbursts, the icf first decreases at nearly constant (slightly decreasing) η. But, as Q_H continues to increase, and before the $icf \rightarrow 1$, η begins to increase at nearly constant icf. Finally, for values of Q_H larger than that for any observed H II regions (*i.e.*, [OIII]/[OI] $\gg 10^3$), η once again decreases and so, too, does the icf ($icf \rightarrow 1$).

4. H II Regions Ionized By Multiple Starbursts

H II regions ionized by soft spectra will have $icf > 1$ and relatively high values of η, while those ionized by harder spectra will have $icf < 1$ and smaller η values. The IT H II regions have relatively small η values ($-0.3 \lesssim \log \eta \lesssim +0.4$; see Fig. 5), confirming the VGS and SJ conclusions that by neglecting the icf (*i.e.*, by *assuming* that the $icf = 1$) IT have likely overestimated the primordial helium abundance. The VGS and SJ results receive further support from Figure 5 where the majority of the IT data points are seen to lie between the zero-age model and the $t = 3.3 - 4.5$ Myr starbursts which have harder spectra and even smaller icfs. However, the spread in the data highlights the likelihood that at least some H II regions may be ionized by spectra from more than one starburst; there is support for this possibility from the Conti & Vacca (1994)

and the Conti, Leitherer, & Vacca (1996) observations of substructure within H II regions. Further support comes from the IT detection of doubly-ionized helium in nearly 3/4 of their H II regions at a level *above* the zero-age prediction, but *below* the predictions of the 3.3 – 4.5 Myr models (see Figs. 4 & 7). Since models of all three of these starbursts predict $icf < 1$, composite models built from these spectra will have intermediate values of η, and $icf < 1$. However, what will happen if, to these spectra, contributions are added from the 2.5 and 5.4 Myr starbursts? Clearly, the resultant H II regions will have intermediate values of η, and an icf which could either be < 1 or > 1.

We have explored two types of composite models to see when H II regions ionized by multiple starbursts will have sufficiently small values of η (and of [OIII]/[OI]), but an icf which exceeds unity. In VGS we studied composite models of *separate* H II regions (ionized by $t = 0$ and 2.5 Myr starbursts) which may be included within the telescope aperture, using various line ratios to exclude such contamination from the IT data (see VGS for details). Here we extend this analysis to combinations of H II regions ionized by $t = 0$ and 5.4 Myr starbursts; starbursts of intermediate age all have $icf < 1$ and will only serve to reduce the icf from its $t = 0$ value. However, before addressing such models, first consider H II regions ionized by the combined spectra of more than one starburst. These multiple starburst possibilities are limitless, so we have chosen to investigate the most "conservative" options: combining a zero-age starburst with either a 2.5 Myr or a 5.4 Myr starburst. Including the 3.3 and/or 4.5 Myr starbursts would only further reduce η and the icf, as well as increase the predicted amount of He^{++} (which may already be too high).

Despite some similarities between the 2.5 Myr and 5.4 Myr spectra, that of the 2.5 Myr starburst is "softer", leading to H II regions with larger values of η and of the icf. The key question is, what is the resulting icf when the contribution from a zero-age starburst (added to a 2.5 Myr starburst) is "large enough" to have reduced η to the IT range ($\log \eta \lesssim 0.4$)? The results, subject to the constraint [OIII]/[OI] $< 10^3$, are shown in Figure 9. It is the [OIII]/[OI] constraint that sets the low η limits and eliminates *any* composite models with $\log \eta < 0.4$ and $icf > 1$, in agreement with our previous conclusions in VGS.

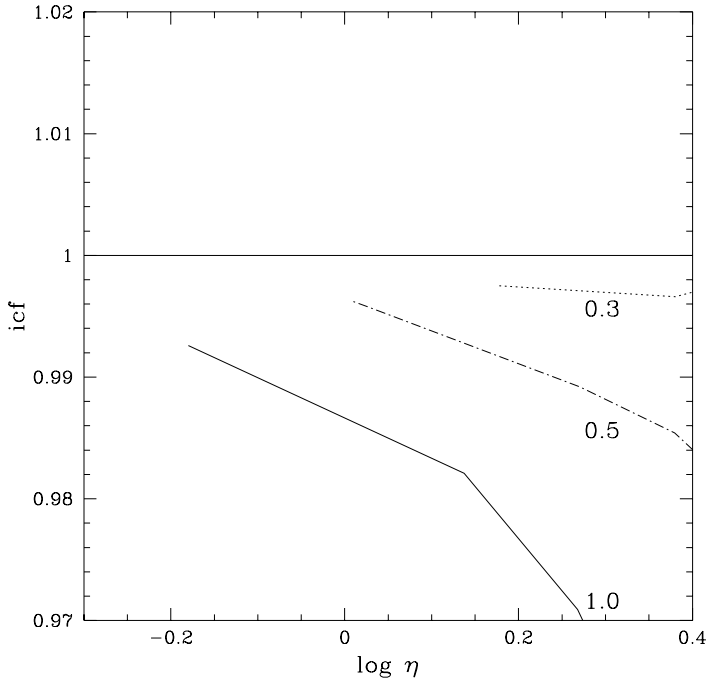

Fig. 9.— The $icf-\log\,\eta$ relation for a series of H II regions ionized by the composite spectra for zero-age and 2.5 Myr starbursts, subject to the constraint that [OIII]/[OI] $< 10^3$. The numbers close to the curves are the fractions of the total flux coming from the zero-age starburst.

The icf versus η relations for several combinations of the $t = 0.0$ and $t = 5.4$ Myr models are shown in Figure 10. Not until the contribution from the aging starburst is some 50 times stronger than that from the infant starburst, does the icf exceed unity (and then, only for $\log\,\eta \gtrsim 0.1$). However, with such a dominant 5.4 Myr old starburst, significant amounts of doubly-ionized helium may be present. The HeII/Hβ predictions for these same composite models are shown in Figure 11. As anticipated, those composite models sufficiently dominated by the 5.4 Myr starburst to have $icf > 1$, will have more HeII than is observed in nearly all of the IT H II regions. Consistent with our earlier results (VGS), as well as those of SJ, it therefore seems unlikely that more than a handful of the IT H II regions can have $icf > 1$.

In agreement with SJ, we note from our exploration of these composite models that the dividing line between $icf < 1$ and > 1 corresponds to a ratio of helium-ionizing to hydrogen-

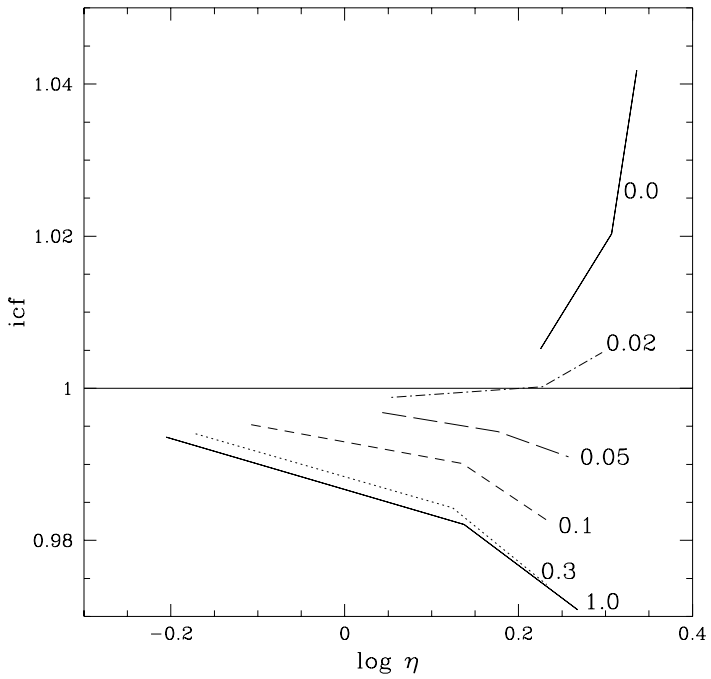

Fig. 10.— The $icf-\log\eta$ relation for a series of H II regions ionized by the composite spectra for zero-age and 5.4 Myr old starbursts, subject to the constraint that [OIII]/[OI] $< 10^3$. For the 5.4 Myr starburst, He/H = 0.075 is adopted. The numbers close to the curves are the fractions of the total flux coming from the zero-age starburst.

ionizing fluxes of ≈ 0.15. Since our spectra for the individual as well as the composite starbursts differ in detail from those of SJ, this result provides supporting evidence that this ratio, and not the detailed shape of the ionizing spectra, is key to determining the sign of $icf - 1$.

For *separate* H II regions, ionized by $t = 0$ and 5.4 Myr starbursts, which may be included within the telescope aperture, the situation is less straightforward. In our exploration of such composite models we have found it possible that the combined H II region can have an $icf > 1$ while satifying $\log\eta \lesssim 0.4$ along with the [OIII]/[OI] and HeII/Hβ constraints. Such models always have $\log\eta \gtrsim 0.25$. A glance at Figure 5 reveals that only five of the forty-one IT H II regions employed in our analysis lie in this range and, of these, only three have observed He^{++}. As a result, only ~ 3 of the IT H II regions ($< 10\%$) might have an $icf > 1$, while still being consistent

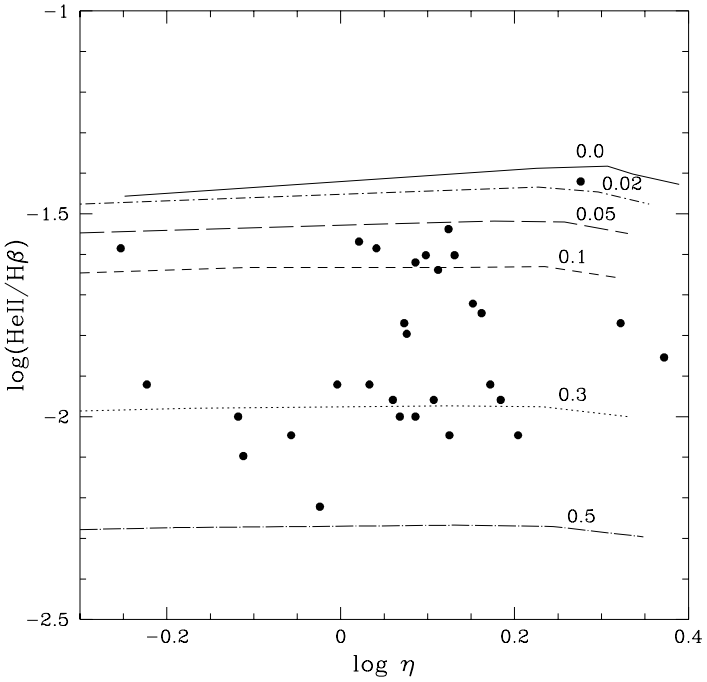

Fig. 11.— The HeII/Hβ−log η relation for H II regions with the same He/H, ionized by the same composite spectra as in Fig. 10 for the zero-age and 5.4 Myr starbursts. The filled circles are the IT data.

with the observed values of η, [OIII]/[OI], and HeII/Hβ.

5. Matter-Bounded Versus Radiation-Bounded

As mentioned earlier, since the [OI]λ6300 emission line is formed in the recombination region, its intensity depends on the optical depth at the Lyman limit, τ_{LL}. As τ_{LL} increases from 1 (matter-bounded) to 10^4 (radiation-bounded), [OI] increases and the [OIII]/[OI] ratio decreases by more than 3 orders of magnitude. Since η is a ratio of ratios, the effect of the Lyman limit optical depth largely cancels and η is relatively insensitive to τ_{LL}.

Images of H II regions show that they are far from being homogeneous, and this suggests that different "sectors" could have different values of τ_{LL}. It is then possible that for the observed

H II regions used in determining Y_P, parts are matter bounded with a very large – local – [OIII]/[OI] ratio, while the remaining radiation bounded sectors have much lower [OIII]/[OI] ratios. Thus, while the observed [OIII]/[OI] ratio might be large, suggesting that no ionization correction need be made (BFM), this may not necessarily be true. Indeed, as has already been seen, for the IT range in [OIII]/[OI], the icf is expected to differ from unity.

To explore the effect of H II regions with matter-bounded pieces, several test cases were run in which the H II region was divided into two sectors, a radiation-bounded part with [OIII]/[OI] $\ll 300$, and a matter-bounded piece with $\tau_{LL} \leq 10$. For matter-bounded sectors with $\tau_{LL} \sim 10$, ratios of [OIII]/[OI] ≥ 300 can be achieved for covering factors of the radiation-bounded sector in the range 0.3 to 0.8. As a result, H II regions might have very large [OIII]/[OI] ratios because they are ionized by very massive starbusts (in which case $icf \rightarrow 1$), or they may have matter-bounded sections and result from much smaller starbursts. For the latter, two-sector models, η shifts to slightly higher values (compared to the corresponding radiation-bounded model) while the icf, although increasing, remains very close to that of the radiation-bounded model. Thus, although partially matter-bounded H II regions might be observed with very high [OIII]/[OI] ratios, suggesting an $icf \rightarrow 1$, the observed value of η provides insurance against being lured into this trap.

The discussion here, as well as that in §3, provides a reminder of the importance of a careful treatment of the recombination transition zone to accurate, quantitative predictions of the model H II region $icf - \eta$ relations. In this connection we note that SJ *assume* that the effects of radiative transfer can be treated in the "On-The-Spot" approximation (OTS). We have tested this assumption and find it to be unjustified. For the spectra of our 0.0, 3.3, and 4.5 Myr models, at fixed η the OTS underestimates the icf (the icf is too small) by a few percent. In contrast, for the 2.5 Myr starburst the OTS overestimates the icf by $\gtrsim 0.25$. For the 5.4 Myr starburst the differences are even more dramatic. For this model, when He/H = 0.083 the $icf - \eta$ relation shown in Fig. 3 is shifted upwards (the icf is overestimated), similar to the shift for the 2.5 Myr model, but in this case by $\gtrsim 0.3$. However, for this same starburst, when He/H = 0.075 the character

of the $icf - \eta$ relation changes completely from that in Fig. 3 to resemble the one for He/H = 0.083 and, the icf is shifted upwards to $icf > 1.25$. Thus, although our results are in excellent *qualitative* agreement with those of SJ, we caution that a careful treatment of radiative transfer is crucial for *quantitatively* accurate, model-predicted H II region icfs.

6. Discussion

In outward appearance, as well as in their internal structure, H II regions evolve as they age. In their infancy H II regions ionized by young, hot, metal-poor stars have ionized helium present in the zone where hydrogen is making the transition from ionized to neutral, resulting in an $icf < 1$. As the starburst ages, the radiation spectrum softens, the icf increases, and in their early youth H II regions will have $icf > 1$. So far, no detectable amounts of doubly-ionized helium will be present. As H II regions enter middle age, the radiation spectrum hardens and the icf decreases, once again dropping below unity. By now the spectrum has enough sufficiently hard photons that detectable amounts of doubly-ionized helium should be present. Finally, as H II regions enter old age, the spectrum softens, the icf increases ($icf > 1$) one last time, and they fade away. But, how does an H II region show its age? Is there a chronometer? The proposed "radiation softness" parameters should be surrogate chronometers but, are they?

As Figure 5 reveals, the [OIII]/[OI] ratio is a very poor chronometer. Notice that for [OIII]/[OI] $\gtrsim 10$, the *same* value of [OIII]/[OI] corresponds to *all* five spectra studied here. While the [OIII]/[OI] ratio provides an excellent measure of the *intensity* of the ionizing radiation, it reveals nothing about the age of the H II region, or the hardness of its spectrum. The situation is better for the Vilchez-Pagel parameter η. Figure 5 suggests that if $\log \eta \gtrsim 0.7$ were observed, then the H II region would likely be dominated by a starburst for which $icf > 1$. Similarly, it is likely that $icf < 1$ for those H II regions with $\log \eta \lesssim -0.1$ (see Fig. 5). However, starbursts of all ages (except 2.5 Myr) could be responsible for H II regions with $-0.1 \lesssim \log \eta \lesssim 0.4$. Of these, the oldest starburst has an $icf > 1$, while all the others have an $icf < 1$. Unfortunately, even in this case (low η), the Vilchez-Pagel radiation softness parameter *alone* is incapable of distinguishing

among starbursts of $t = 0.0$, 3.3, and 4.5 Myr, even though the latter two, older starbursts have very different spectra from the youngest one.

At the same time that Figure 5 exposes the inadequacy of the [OIII]/[OI] ratio, and the deficiencies of η, it suggests that η and [OIII]/[OI] *in combination* might provide a more useful gauge of H II region ages by helping to separate the effects of "hard" versus "soft" spectra (which determine whether $icf < 1$ or > 1) from those related to the intensity of the starburst (which determines by *how much* the icf will differ from unity). In addition, for $\log \eta \lesssim 0.5$, the presence or absence of He^{++} may help to discriminate between infancy (no observable He^{++} at $t \approx 0$) and maturity (detectable He^{++} present for $3 \lesssim t \lesssim 5$ Myr); see Fig. 4. For example, H II regions with [OIII]/[OI] $\gtrsim 150$ and $0.3 \lesssim \log \eta \lesssim 0.5$ are likely ionized by an old (~ 5.4 Myr) starburst and should have detectable He^{++}, while those with the same large values of [OIII]/[OI], but with $-0.1 \lesssim \log \eta \lesssim 0.2$, should be dominated by a very young ($t \approx 0$) starburst and they should have no observable He^{++}. With reference to Figs. 3, 5, and 6, this approach may be applied to the IT data.

Of the 41 IT H II regions in our data set, 36 have $\log \eta \lesssim 0.25$ (see Fig. 5) and are likely ionized by radiation with spectra similar to those of our $t = 0.0$, 3.3, or 4.5 Myr starbursts. For these H II regions, $icf < 1$. Of the remaining five H II regions, only three have He^{++} detected; only these three are likely to have significant or dominant contributions from a spectrum similar to that of our 5.4 Myr starburst for which $icf > 1$. It seems likely then that for more than 90% (38/41) of the IT H II regions, $icf < 1$ and Y < Y(IT). This dominance of $icf < 1$ is not at all surprising when considering that an H II region spends most of its life ionized by a hard radiation spectrum with $Q(He^0)/Q(H^0) > 0.15$ (see Fig. 2). To estimate the magnitude of the ionization correction it is necessary to use the available data for *both* $\log \eta$ *and* $\log$([OIII]/[OI]) since for the three starbursts with hard spectra, the model-predicted icfs vary significantly (see Fig. 3) over the range in η covered by the IT data ($-0.3 \lesssim \log \eta \lesssim 0.25$). However, for $\log([OIII]/[OI]) \gtrsim 1.7$ (see Fig. 5), the icfs for these three starburst models are nearly identical and, for $\log([OIII]/[OI]) \lesssim 2.9$, they do differ from unity (see Fig. 6). As a result of this comparison, we conclude that for $\sim 38/41$ of the

IT H II regions, $0.95 \lesssim icf \lesssim 0.99$. Since the IT helium abundance determinations range from Y ≈ 0.24 to Y ≈ 0.26, this suggests a correction to Y_P(IT) in the range $0.002 \lesssim -\Delta Y \lesssim 0.010$, in excellent agreement with the SJ estimate of a $\sim 2-4$ % overestimate in the helium abundance, corresponding to $0.005 \lesssim -\Delta Y \lesssim 0.010$. Approximating our correction as $\Delta Y \approx -0.006 \pm 0.002$ and combining it in quadrature with the IT primordial helium estimate of Y_P(IT)$= 0.244 \pm 0.002$, leads to a revised estimate of $Y_P = 0.238 \pm 0.003$.

7. Conclusions

The history of the study of the helium-hydrogen icf extends over several decades (see VGS for references to early work) and the different model assumptions may have obscured the fact that all such studies reach the same general conclusions. H II regions ionized by massive, intense starbursts will be large and, when radiation bounded, the transition zone from ionized to neutral gas is relatively thin compared to the overall size of the H II region. For such H II regions the $icf \rightarrow 1$. As the intensity of the starburst diminishes, the relative size of the transition zone increases and the icf deviates from unity. Whether the deviation will be $icf < 1$ or $icf > 1$ is determined by the relative hardness of the *spectrum* of the starburst, *not* by its intensity. Although there will be some quantitative differences among the predicted icfs depending on the details of the spectra adopted (*e.g.*, compare VGS, BFM, and SJ), it is clear that the ratio of helium-ionizing to hydrogen-ionizing photons is key to determining whether the $icf < 1$ or > 1. Thus, although the spectra adopted here for starbursts of differing ages differ somewhat from the corresponding spectra in SJ, we agree with them that there is a "critical" value of $Q(He^0)/Q(H^0)$ ≈ 0.15 separating H II regions with $icf < 1$ from those with $icf > 1$. An ideal radiation softness parameter would provide a unique reflection of this ratio. The Vilchez-Pagel parameter η, although imperfect, is a valuable surrogate. However, even when it can be determined that the $icf < 1$ (or, > 1), the amount by which the icf deviates from unity depends on the intensity of the radiation spectrum. For more intense (more massive) starbursts, η decreases, [OIII]/[OI] increases, and the $icf \rightarrow 1$. However, the majority of the H II regions used to infer the primordial helium abundance

have values of η and [OIII]/[OI] which lie in those ranges where the models suggest significant (*i.e.*, few percent) deviations of the icf from unity. Note that for an uncorrected helium mass fraction in the range Y $\approx 0.24 - 0.26$ (IT), a 3% deviation in the icf from unity corresponds to a change in helium abundance of order 0.006, three times as large as the IT error on their inferred primordial helium mass fraction. Indeed, in our previous analysis we estimated that the IT value of $Y_P = 0.244 \pm 0.002$ needed to be reduced by approximately 0.003 (VGS). The analysis presented here, in agreement with that of SJ, strengthens this conclusion and suggests that the reduction may be even larger.

The IT primordial helium estimate ($Y_P = 0.244 \pm 0.002$) is already somewhat low in comparison to the BBN-predicted value based on the baryon density inferred from the deuterium observations of O'Meara *et al.* (2001): for D/H $= 3.0 \pm 0.4 \times 10^{-5}$, $\Omega_B h^2 = 0.020 \pm 0.002$, and $Y_P(\mathrm{BBN; D/H}) = 0.247 \pm 0.001$. If, instead, the CMB estimate of the baryon density is used, $\Omega_B h^2 = 0.022 \pm 0.002$ (*e.g.*, Kneller *et al.* 2001 and references therein), the predicted primordial helium abundance is even larger: $Y_P(\mathrm{BBN; CMB}) = 0.248 \pm 0.001$. Here we have corrected the IT estimate for unobserved neutral hydrogen and/or helium, concluding that $Y_P = 0.238 \pm 0.003$, thus increasing the tension between the expected and inferred primordial helium abundances. Almost certainly, the discussion here will not be the final word on the primordial abundance of helium.

Acknowledgments

In Brazil the work of S.M.V. and R.G. is partially supported by grants from CNPq (304077/77-1 and 306122/88-0), from FAPESP (00/06695-0), and from PRONEX/FINEP (41.96.0908.00); in the U.S. the work of G.S. is supported at The Ohio State University by DOE grant DE-AC02-76ER-01545. Some of this work was done while S.M.V. was visiting the OSU Physics Department and while G.S. was visiting IAGUSP and they wish to thank the respective host institutions for hospitality.

References

Armour, M.-H., Ballantyne, D.R., Ferland, G.J., Karr, J. & Martin, P.G. 1999, PASP, 111, 1251

Bahcall, J.N., Pinsonneault, M.H., & Basu, S. 2001, ApJ, 555, 990

Ballantyne, D.R., Ferland, G.J., & Martin, P.G. 2000, ApJ, 536, 773 (BFM)

Conti, P.S. & Vacca, W.D. 1994, ApJL, 494, L97

Conti, P.S., Leitherer, C., & Vacca, W.D. 1996, ApJL, 461, L87

Cid-Fernandes, R., Dottori, H., Gruenwald, R., & Viegas, S.M. 1992, MNRAS, 255, 165

Gruenwald, R. & Viegas, S.M. 1992, ApJS, 78, 153 (AANGABA)

Gruenwald, R. & Viegas, S.M. 2000, ApJ, 543, 889

Izotov, Y.I., Thuan, T.X., & Lipovetsky, V.A. 1994 ApJ, 435, 647 (ITL)

Izotov, Y.I., Thuan, T.X., & Lipovetsky, V.A. 1997, ApJS, 108, 1 (ITL)

Izotov, Y.I. & Thuan, T.X. 1998, ApJ, 500, 188 (IT)

Kneller, J.P., Scherrer, R.J., Steigman, G., & Walker, T.P. 2001, Phys. Rev. D, In Press (astro-ph/0101386)

Olive, K.A., Skillman, E. & Steigman, G. 1997, ApJ, 483, 788 (OSS)

Olive, K.A., & Steigman, G. 1995, ApJS, 97, 49 (OS)

Olive, K.A., Steigman, G., & Walker, T.P. 2000, Physics Reports, 333-334, 389

O'Meara, J.M. *et al.* 2001, ApJ, 552, 718

Pagel, B.E.J., Simonson, E.A., Terlevich, R.J. & Edmunds, M. 1992, MNRAS, 255, 325

Peimbert, M., Peimbert, A., & Ruiz, M.T. 2000, ApJ, 541, 688

Sauer, D. & Jedamzik, K. 2001, preprint (astro-ph/0104392) (SJ)

Skillman, E.D. 1989, ApJ, 347, 883

Stasinska, G. 1990, A&A Suppl., 83, 501

Viegas, S.M., Gruenwald, R., & Steigman, G. 2000, ApJ, 531, 813 (VGS)

Vilchez, J.M. & Pagel, B.E.J. 1988, MNRAS, 231, 257